MATCH
Communications in Mathematical and in Computer Chemistry

MATCH Commun. Math. Comput. Chem. **66** (2011) 751-764

ISSN 0340 - 6253

Möbius Systems and the Estrada Index

Patrick W. Fowler

University of Sheffield, Department of Chemistry, Sheffield S3 7HF, UK

P.W.Fowler@sheffield.ac.uk

(Received June 17, 2010)

Abstract

Where the characteristic polynomial of a graph G is a product or quotient of characteristic polynomials of graphs $\{H_i\}$, the Estrada Index (sum of exponentials of eigenvalues), $EE(G)$, is evidently a linear combination of the $EE(H_i)$. In particular, this leads to connections between Estrada Indices for σ- and π-bonded Möbius-twisted molecular frameworks, and implies that non-bipartite Möbius graphs have a bipartivity index that exceeds the value of unity for bipartite graphs. As examples of Möbius cycles, ladders and polyacenes all illustrate, the effect of the half twist washes out rapidly, and the linear asymptotic limit of $EE(G)$ is reached for small numbers of vertices.

1 Introduction

The Estrada Index has been proposed as a measure of branching, centrality and related properties of large graphs[1–3] and has attracted attention in chemical and mathematical graph theory.[4,5] It is calculated for a graph G of order n by taking the sum of exponentials of eigenvalues of the adjacency matrix $\mathbf{A}(G)$:

$$EE(G) = \sum_{i=1}^{n} e^{\lambda_i} = \sum_{i=1}^{n} Tr\{e^{\mathbf{A}}\}, \tag{1}$$

with convergent expansion

$$EE(G) = \sum_{i=1}^{\infty} \frac{\mu^{(k)}}{k!}, \tag{2}$$

where $\mu^{(k)}$ is the k-th spectral moment: $\mu^{(k)} = \sum_{i=1}^{n} \lambda_i^k$. Evidently, as the eigenvalues $\{\lambda_i\} \equiv Sp(G)$ are the roots of the characteristic polynomial

$$\varphi(G, x) = \det(\lambda \mathbf{1} - \mathbf{A}G), \tag{3}$$

any factorisations of φ imply additivity relations for $EE(G)$. A related invariant is the bipartivity index[6]

$$\beta(G) = \frac{1}{2} \sum_{i=1}^{n} (e^{\lambda_i} + e^{-\lambda_i}) / \sum_{i=1}^{n} e^{\lambda_i}. \tag{4}$$

For making links between $EE(G)$ and $\beta(G)$, it is also useful to define

$$FF(G) = \sum_{i=1}^{n} e^{-\lambda_i}, \tag{5}$$

with $EE(G) = FF(G)$, $\beta(G) = 1$ for bipartite graphs, and $EE(G) > FF(G)$, $\beta(G) < 1$ for (unweighted) non-bipartite graphs. By definition, for all graphs:

$$2\beta(G)EE(G) = EE(G) + FF(G) \tag{6}$$

A number of bounds and approximations for $EE(G)$ are known,[5] and in particular relations have been derived for $EE(G)$, in the case that G is one of various product graphs.[7] Empirical evidence suggests that $EE(G)$ is essentially linear for classes of graphs with a fixed relation between order n and size m. For example, cycles and paths have asymptotic approximations[4]

$$EE(C_n) \approx nI_0, \qquad EE(P_n) \approx (n+1)I_0 - \cosh(2), \tag{7}$$

with[8]

$$I_0 = \sum_{k=1}^{\infty} \frac{1}{(k!)^2} = 2.279585302336067\ldots \tag{8}$$

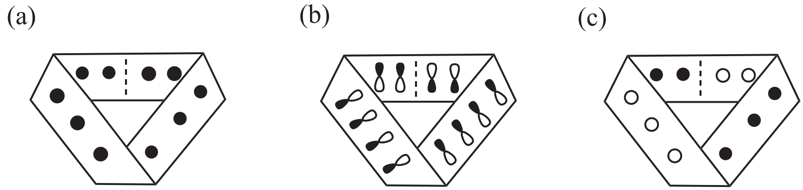

Figure 1: Phase relations for σ- and π-bonded systems embedded on the Möbius strip: (a) σ-bonded array of s orbitals; π-bonded array of overlapping p orbitals (b) lying parallel *in* and (c) locally *perpendicular to* the Möbius strip surface. In (b) and (c), there is an unavoidable phase interruption at the seam of the Möbius strip (shown dotted).

Both approximations are already accurate at small n. Fullerene graphs provide another example of excellent linearity,[9] with a slope within a few percent of the value of $\frac{1}{3}\sinh(3) \approx 3.33929\ldots$ predicted for cubic graphs by a general approximation in terms of n and m.[10]

The present note points out some simple consequences of combination relations for $EE(G)$ in the case where G is the skeleton of a molecular system with Möbius topology. For several interesting classes of molecular graph, it turns out that $EE(G)$ is sensitive to the presence of the half-twist for small values of n only, and otherwise converges rapidly to a linear asymptotic expression.

2 Möbius graphs

One connection of graph theory with molecular electronic structure is through the Hückel model, where diagonalisation of the adjacency matrix $\mathbf{A}(G)$ gives a qualitative description of energy levels and distribution of valence electrons in the molecular framework with skeleton G.[11] The model is usually applied to π systems, where bonding arises from sideways overlap of p orbitals, but can also be applied to σ systems, where overlap is end-on. For π systems with Möbius topology, an edge in each non-contractible cycle of the embedded graph G is given weight -1, to account for the phase interruption of overlap across the 'seam' of the underlying the Möbius strip.[12–15] This is true, whether the locally parallel p orbitals are lying in or perpendicular to the surface. No re-weighting of edges is needed for σ systems (Figure 1). The two weighting schemes for an underlying graph G are denoted by πG and σG, respectively.

A general relation between $EE(\sigma G)$ and $EE(\pi G)$ comes from the fact that the Möbius strip is doubly covered by the cylinder.[16] If a cylindrical surface is built from two copies of the Möbius strip using the gluing rules illustrated in Figure 2, each point i of the starting strip generates a pair of images $i^\star$ and $i^{\star\star}$, related by inversion on the cylinder.

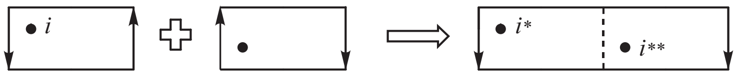

Figure 2: Double-cover relation for Möbius strip and cylinder surfaces. The arrows indicate the gluing rules at the seams for the two copies of the Möbius strip making up the cylinder surface populated with antipodal image points.

Likewise, a graph $G_{1/2}$ embedded on the Möbius strip is doubly covered by a centrosymmetric graph G_1 embedded on the cylinder. It is easy to show[15] that each eigenvector of the weighted adjacency matrix $\mathbf{A}(\pi G_{1/2})$ corresponds to an *ungerade* eigenvector of $\mathbf{A}(G_1)$, and each of $\mathbf{A}(\sigma G_{1/2})$ to a *gerade* eigenvector, where labels denote vectors that are *odd* or*even* under inversion, respectively. Hence, the double-cover relationship between cylinder and Möbius strip implies a particular factorisation of the characteristic polynomial,

$$\varphi(G_1, x) = \varphi(\sigma G_{1/2}, x) \times \varphi(\pi G_{1/2}, x), \tag{9}$$

and therefore partition of the spectrum into σ- and π-bonding halves,

$$Sp(G_1) = Sp(\sigma G_{1/2}) \cup Sp(\pi G_{1/2}), \tag{10}$$

which leads to some easy mini-theorems.

Theorem 1 *The π and σ versions of a graph $G_{1/2}$ have addition relations for the Estrada and bipartivity indices:*

$$EE(G_1) = EE(\sigma G_{1/2}) + E(\pi G_{1/2}), \tag{11}$$

$$\beta(G_1)EE(G_1) = \beta(\sigma G_{1/2})EE(\sigma G_{1/2}) + \beta(\pi G_{1/2})E(\pi G_{1/2}). \tag{12}$$

Proof. Directly from definitions (1) and (4).

A straightforward deduction is

Theorem 2 *The π and σ versions of a graph $G_{1/2}$ have*

$$EE(\sigma G_{1/2}) \geq EE(\pi G_{1/2}). \tag{13}$$

Proof. The spectral moment $\mu^{(k)}$ of a graph is equal to the number of self-returning walks of length k, each weighted by the product of their edge weights. Moments at each k are pairwise equal for $\sigma G_{1/2}$ and $\pi G_{1/2}$, except where some self-returning walk of length k in $\pi G_{1/2}$ includes an odd number of negatively weighted edges. Each such walk adds $2k$ to the k-th moment for the σ graph and subtracts $2k$ for the π graph. Such walks are present unless $G_{1/2}$ is bipartite. Hence, by (2), the result follows. $\square$

The first divergence of $EE(\sigma G_{1/2})$ and $EE(\pi G_{1/2})$ occurs at $\mu^{(k')}$, where k' is the size of the smallest noncontractible cycle, and, with n_w such cycles, gives leading term

$$EE(\sigma G_{1/2}) - EE(\pi G_{1/2}) = \frac{4n_w}{(k'-1)!} + \dots \tag{14}$$

consistent with rapid convergence to equality as the order of the graph and length of the relevant cycle(s) increase.

Another observation arises from the fact that the spectra of weighted graphs $\sigma G_{1/2}$ and $\pi G_{1/2}$ are often connected by a symmetry relation over and above the double-cover relation (10):

Theorem 3 *If G_1 is bipartite and $G_{1/2}$ non-bipartite, the two spectra are mirror-paired, in the sense that for every eigenvalue λ in Sp$(\sigma G_{1/2})$ there is an eigenvalue $-\lambda$ with the same multiplicity in Sp$(\pi G_{1/2})$.*

Proof. For the mirror property to hold, it is necessary that G_1 be bipartite, since its eigenvalues must be paired, and it is also necessary that $G_{1/2}$ be non-bipartite, from the non-degeneracy of the Perron eigenvalue of G_1. Sufficiency follows by supposing G_1 to be bipartite and $G_{(1/2)}$ non-bipartite, and considering their subgraphs H_i and $H_{1/2}$ obtained by deleting all seam-crossing edges. H_i is bipartite and consists of two disconnected copies of $H_{1/2}$, which is therefore also bipartite. Make a bipartite colouring of the vertices $H_{1/2}$ and transfer it to $G_{1/2}$. The edges of $G_{(1/2)}$ that were deleted to make $H_{1/2}$ now connect vertices of like colour. If vertices of $G_{1/2}$ are now labelled with the entries in the eigenvector of $\mathbf{A}(\sigma G_{1/2})$ that corresponds to eigenvalue λ, an eigenvector of $\mathbf{A}(\pi G_{1/2})$ corresponding to eigenvalue $-\lambda$ can be constructed: change edge-weights to -1 for all like-like pairs and flip the signs of the entries on all vertices in one colour class. □

Theorem 4 *Whenever it is true that* $Sp(\sigma G_{1/2}) = Sp(\pi G_{1/2})$*, it follows that*

$$EE(\sigma G_{1/2}) = FF(\pi G_{1/2}) \quad FF(\sigma G_{1/2}) = EE(\pi G_{1/2}) \quad FF(\pi G_{1/2}) > EE(\pi G_{1/2}) \tag{15}$$

with the result that

$$\beta(\sigma G_{1/2})EE(\sigma G_{1/2}) = \beta(\pi G_{1/2})EE(\pi G_{1/2}) \tag{16}$$

and

$$\beta(\pi G_{1/2}) > 1 > \beta(\sigma G_{1/2}) \tag{17}$$

This last result for β has the unsettling implication that non-bipartite π-bonded Möbius structures can be nominally 'more bipartite' than bipartite graphs. As with $EE(\pi G_{1/2}) - EE(\sigma G_{1/2})$, in fact the difference $\beta(\pi G_{1/2}) - \beta(\sigma G_{1/2})$ typically converges rapidly to zero as a function of graph order, and for the same reasons.

3 Examples

3.1 Möbius cycles

The Möbius cycle (Möbius annulene) was introduced as a model of twisted cyclic polyenes[12] and pericyclic transition states.[13] It consists of a cycle with one edge weighted by -1. The characteristic polynomials for C_n and M_n are[11,14]

$$\varphi(C_n, x) = 2\cos(n\tau) - 2 \tag{18}$$

$$\varphi(M_n, x) = 2\cos(n\tau) + 2 \tag{19}$$

with $\tau = \cos^{-1}(x/2)$, and the eigenvalues are drawn from the set

$$\lambda_k = 2\cos(k\pi/n) \quad \text{with} \quad k = 0, \ldots 2n-1 \tag{20}$$

where even values of k give eigenvalues of C_n and odd values give eigenvalues of M_n. The double-cover relation (10) implies

$$\varphi(C_{2n}, x) = \varphi(C_n, x) \times \varphi(M_n, x) \tag{21}$$

and

$$EE(M_n) = EE(C_{2n}) - EE(C_n). \tag{22}$$

The mirror relationship of $\mathrm{Sp}(C_n)$ and $\mathrm{Sp}(M_n)$ holds for odd n, as can be seen from (20). As implied by the moment expansion,

$$EE(C_n) \geq \frac{1}{2} EE(C_{2n}) \geq EE(M_n) \tag{23}$$

and

$$\beta(M_n) = 1 = \beta(C_n) \qquad \text{for} \quad \text{odd} \quad n, \tag{24}$$

$$\beta(M_n) > 1 > \beta(C_n) \qquad \text{for} \quad \text{even} \quad n. \tag{25}$$

n	$EE(C_n)$	$EE(M_n)$	$\beta(C_n)$	$\beta(M_n)$
3	8.1248149813	5.5718989402	0.8428938968	1.2290885090
4	9.5243913822	8.7127342264	1.0000000000	1.0000000000
5	11.4961863219	11.2996727354	0.9914530967	1.0086955433
6	13.6967139214	13.6583097607	1.0000000000	1.0000000000
7	15.9602420645	15.9539521685	0.9998029511	1.0001971266
8	18.2371256086	18.2362392288	1.0000000000	1.0000000000
9	20.5163225164	20.5162129257	0.9999973292	1.0000026708
10	22.7958590573	22.7958469894	1.0000000000	1.0000000000
11	25.0754389246	25.0754377268	0.9999999761	1.0000000239
12	27.3550236821	27.3550235739	1.0000000000	1.0000000000
13	29.6346089349	29.6346089259	0.9999999998	1.0000000002
14	31.9141942330	31.9141942324	1.0000000000	1.0000000000
15	34.1937795351	34.1937795350	1.0000000000	1.0000000000

Table 1: Estrada and bipartivity indices of the small cycles and Möbius cycles.

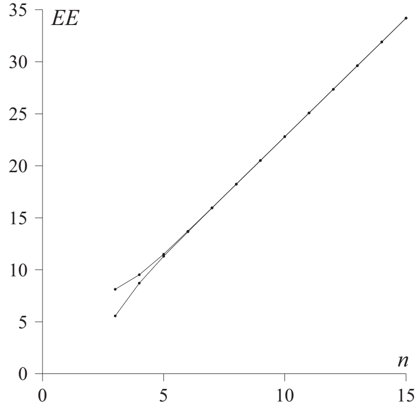

Figure 3: Estrada index for cycles and Möbius cycles. The upper curve represents cycles and the lower Möbius cycles.

In practice, convergence to equality between C_n and M_n for both β and EE is extremely rapid (Table 1 and Figure 3) and for all practical purposes $EE(M_n) \approx EE(C_n) \approx nI_0$ from $n = 3$ onwards.

3.2 Ladders and Möbius Ladders

The Ladder graph, L_n, is the Cartesian product $C_{n/2} \times K_2$ and is the skeleton of the n-gonal prism. When embedded equilaterally in the cylinder, it has $(n/2)$ square faces forming a cylindrical strip. A canonical numbering of vertices has vertices 1 to $n/2$ in one $C_{n/2}$ cycle, vertices $n/2+1$ to n in the other, and adjacencies $i \sim i + n/2$ to $i = 1, n/2$ to complete the squares.

The characteristic polynomial is

$$\varphi(L_n, x) = \varphi(C_{n/2}, x+1) \times \varphi(C_{n/2}, x-1) \tag{26}$$

and hence the spectrum consists of two offset copies of $\mathrm{Sp}(C_(n/2))$, implying

$$EE(L_n) = (e + e^{-1})EE(C_{n/2}) \tag{27}$$

and

$$\beta(L_n) = \beta(C_{n/2}) \tag{28}$$

again with rapid convergence to the asymptotic limit

$$EE(L_n) \approx (e + e^{-1})I_0 n \approx 3.517558\ldots\, n \tag{29}$$

The expression (29) is a particular case of the theorem for Cartesian products that the Estrada Index of the product $G \times H$ is the product of the indices $EE(G) \times EE(H)$.[7]

The Möbius Ladder, ML_n, is notionally derived by cutting the cylindrical strip of the conventional ladder graph of squares and rejoining with a half-twist. In the numbering scheme given for L_n, this could be done by breaking edges $1 \sim n/2$ and $n/2+1 \sim n$ and making $1 \sim n$ and $n/2 \sim n/2+1$. With all edge weights equal to $+1$, this is the graph mainly considered in mathematical graph theory.[7,17] With weights of -1 on the two new edges, it is the graph appropriate to π-bonded frameworks.

L_n is bipartite iff $n/2$ is even, and ML_n is bipartite iff $n/2$ is odd. The spectra $\mathrm{Sp}(\sigma ML_n)$ and $\mathrm{Sp}(\pi ML_n)$ have the mirror property iff $n/2$ is even, with the result that

$$\beta(\pi ML_n) > 1 > \beta(\sigma ML_n). \tag{30}$$

n	$EE(L_n)$	$EE(\sigma ML_n)$	$EE(\pi ML_n)$	$\beta(L_n)$	$\beta(\sigma ML_n)$	$\beta(\pi ML_n)$
6	25.0744893181	24.1353239916	18.1349440340	0.8428938968	1.0000000000	1.0000000000
8	29.3938078004	29.0952158196	27.1874949031	1.0000000000	0.9672159002	1.0350845292
10	35.4790849751	35.4067916667	34.9449056639	0.9914530967	1.0000000000	1.0000000000
12	42.2702680255	42.2561399243	42.1658746933	1.0000000000	0.9989319276	1.0010703588
14	49.2558809134	49.2535669900	49.2387832035	0.9998029511	1.0000000000	1.0000000000
16	56.2827107227	56.2823846417	56.2803012925	1.0000000000	0.9999814920	1.0000185087
18	63.3166799453	63.3166396291	63.3163820469	0.9999973292	1.0000000000	1.0000000000
20	70.3516973306	70.3516928910	70.3516645267	1.0000000000	0.9999997984	1.0000002016
22	77.3868484280	77.3868479874	77.3868451722	0.9999999761	1.0000000000	1.0000000000
24	84.4220146176	84.4220145778	84.4220143235	1.0000000000	0.9999999985	1.0000000015
26	91.4571823354	91.4571823321	91.4571823110	0.9999999998	1.0000000000	1.0000000000
28	98.4923501935	98.4923501932	98.4923501916	1.0000000000	1.0000000000	1.0000000000
30	105.5275180634	105.5275180634	105.5275180633	1.0000000000	1.0000000000	1.0000000000

Table 2: Estrada and bipartivity indices of ladders and Möbius ladders

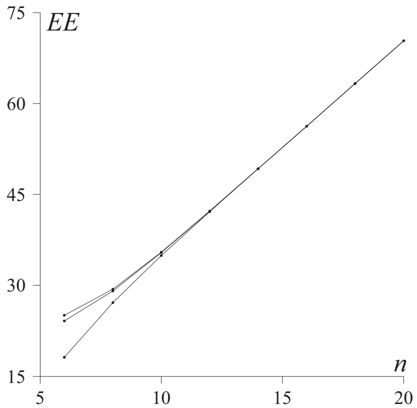

Figure 4: Estrada index for cylindrical and Möbius ladders. Upper, middle and lower curves represent cylindrical, σ- and π-Möbius ladders, respectively.

The double-cover property implies

$$\mathrm{Sp}(L_{2n}) = \mathrm{Sp}(\sigma ML_n) + \mathrm{Sp}(\pi ML_n) \tag{31}$$

$$EE(L_{2n}) = EE(\sigma ML_n) + EE(\pi ML_n) \tag{32}$$

but factorisation of the respective characteristic polynomials gives explicit forms[18]

$$\varphi(\sigma ML_n, x) = \varphi(C_{n/2}, x-1) \times \varphi(M_{n/2}, x+1), \tag{33}$$

$$\varphi(\pi ML_n, x) = \varphi(C_{n/2}, x+1) \times \varphi(M_{n/2}, x-1), \tag{34}$$

from which the spectra are seen to be shifted versions of $\mathrm{Sp}(C_{n/2})$ and $\mathrm{Sp}(M_{n/2})$, and

$$EE(\sigma ML_n) = e^{-1}EE(C_n) + (e - e^{-1})EE(C_{n/2}), \tag{35}$$

(in agreement with the expression from a theorem for EE of graph products[7]), and

$$EE(\pi ML_n) = eEE(C_n) + (e^{-1} - e)EE(C_{n/2}). \tag{36}$$

The indices of the various ladders are therefore ranked

$$EE(\pi ML_n) < \frac{1}{2}EE(L_{2n}) < EE(\sigma ML_n) < EE(L_n), \tag{37}$$

with rapid convergence (Table 2, Figure 4) to

$$EE(\pi ML_n) \approx \frac{1}{2}EE(L_{2n}) \approx EE(\sigma ML_n) \approx EE(L_n) \approx (e + e^{-1})I_0\, n \tag{38}$$

Bipartivities obey

$$\beta(\pi ML_n) = 1 = \beta(\sigma ML_n) \qquad \text{for} \quad \text{odd} \quad n/2, \tag{39}$$

$$\beta(\pi ML_n) = 1 = \beta(\sigma ML_n) \qquad \text{for} \quad \text{even} \quad n/2, \tag{40}$$

with rapid convergence to equality of $\beta \approx 1$ for all three series (Table 2).

3.3 Cyclic polyacenes

The cyclic polyacene graphs PA_n are analogues of the ladder graphs in which the building blocks are fused hexagons rather than squares. They are models for hypothetical cyclic and Möbius benzenoid systems. Untwisted polyacenes can be constructed by subdividing edges of the two $C_{n/2}$ cycles of the ladder graph, and are hence bipartite for all n, with $n/4$ hexagonal faces and two faces of size $n/2$ when embedded on the cylinder. The

n	$EE(PA_n)$	$EE(\sigma MPA_n)$	$EE(\pi MPA_n)$	$\beta(\sigma MPA_n)$	$\beta(\pi MPA_n)$
12	33.2805988574	33.2568995393	33.2161774318	0.9993877645	1.0006129861
16	44.3163977555	44.3158527779	44.3149163527	0.9999894346	1.0000105656
20	55.3942444679	55.3942370659	55.3942243473	0.9999998852	1.0000001148
24	66.4730769711	66.4730769048	66.4730767910	0.9999999991	1.0000000009
28	77.5519229900	77.5519229896	77.5519229889	1.0000000000	1.0000000000
32	88.6307691306	88.6307691306	88.6307691306	1.0000000000	1.0000000000
36	99.7096152719	99.7096152719	99.7096152719	1.0000000000	1.0000000000
40	110.7884614132	110.7884614132	110.7884614132	1.0000000000	1.0000000000
44	121.8673075545	121.8673075545	121.8673075545	1.0000000000	1.0000000000
48	132.9461536958	132.9461536958	132.9461536958	1.0000000000	1.0000000000
52	144.0249998372	144.0249998372	144.0249998372	1.0000000000	1.0000000000
56	155.1038459785	155.1038459785	155.1038459785	1.0000000000	1.0000000000
60	166.1826921198	166.1826921198	166.1826921198	1.0000000000	1.0000000000

Table 3: Estrada and bipartivity indices of polyacenes and Möbius polyacenes

Möbius polyacene MPA_n is constructed by twisting and re-gluing the hexagon strip in the obvious way, and is non-bipartite for all n odd. Characteristic polynomials of the polyacenes are not simple products of characteristic polynomials for smaller graphs,[15,19] but the double-cover and spectral mirror relationships still apply, so that

$$EE(\pi MPA_n) \approx \frac{1}{2}EE(PA_{2n}) \approx EE(\sigma MPA_n) \approx EE(PA_n) \approx K\,n \tag{41}$$

with K apparently slightly smaller than the generic (n, m) estimate[10] of ~ 2.81 for $m = 5n/4$, and

$$\beta(\pi MPA_n) > 1 > \beta(\sigma MPA_n). \tag{42}$$

As the numerical values show (Table 3, Figure 5), the effect of the Möbius half-twist is essentially negligible, even for the smallest polyacene systems.

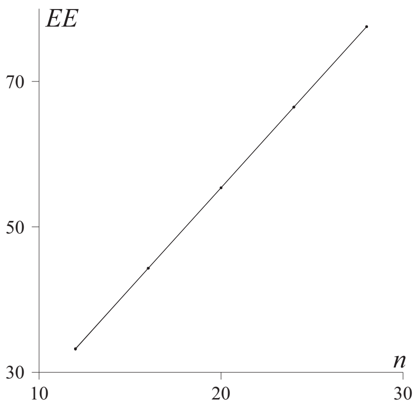

Figure 5: Estrada index for cylindrical and Möbius polyacenes.

4 Concluding remarks

Characteristic relationships have been demonstrated for Estrada and bipartivity indices of graphs embedded on the Möbius strip. The examples tend show that the standard Estrada Index is insensitive to the presence of a half-twist in a graph. This can be traced to the relatively large ring size at which the weights on the special 'seam-crossing' edges first begin to influence spectral moments. If it is required to give better discrimination for Möbius character, then the 'zooming' technique described by Estrada,[20] in which denominator factorials in the expansion are allowed to 'slide' to emphasise the contributions of longer or shorter cycles, offers a possible direction for further investigation. Analysis of the mean and variance of the Estrada Index, as carried out for 3-regular graphs,[21] may also give some insight into differences between Möbius and non-Möbius graphs.

References

[1] E. Estrada, Characterization of 3D molecular structure, *Chem. Phys. Lett.* **319** (2000) 713–718.

[2] E. Estrada, Characterization of the folding degree of proteins, *Bioinformatics* **18** (2002) 697–704.

[3] E. Estrada, Characterization of the amino acid contribution to the folding degree of proteins, *Proteins* **54** (2004) 727-737.

[4] I. Gutman, A. Graovac, Estrada index of cycles and paths, *Chem. Phys. Lett.* **436** (2007) 294–296.

[5] H. Deng, S. Radenković, I. Gutman, The Estrada index, in: D. Cvetković, I. Gutman (Eds.), *Applications of Graph Spectra*, Math. Inst., Belgrade, 2009, pp. 123–140.

[6] T. Došlić, Bipartivity of fullerene graphs and fullerene stability, *Chem. Phys. Lett.* **412** (2005) 336–340.

[7] G. H. Fath–Tabar, A. R. Ashrafi, I. Gutman, Note on Estrada and L-Estrada indices of graphs, *Bull. Acad. Serbe Sci. Arts (Cl. Math. Natur.)* **139** (2009) 1–16.

[8] Quoted to 8 places of decimals in Ref. 4, but available to 15 in e.g., Plouffe's Inverter (see http://pi.lacim.uquam.ca/). Combined with more accurate eigenvalues, this extra precision shows that the approximation is even better than suggested in Ref. 4.

[9] P. W. Fowler, A. Graovac, The Estrada index and fullerene isomerism, in: A. Graovac, O. Ori, F. Cataldo (Eds.), *Mathematics and Chemistry of the Fullerenes*, to appear in the series *Carbon Materials Chemistry and Physics*, Springer, New York.

[10] I. Gutman, S. Radenković, A. Graovac, D. Plavšić, Monte Carlo approach to Estrada index, *Chem. Phys. Lett.* **446** (2007) 233–236. (The general expression is $n/k \sinh(k)$ with $k = \sqrt{6m/n}$; see equation (11).)

[11] I. Gutman, O. E. Polansky, *Mathematical Concepts in Organic Chemistry*, Springer–Verlag, Berlin, 1986.

[12] E. Heilbronner, Hückel molecular orbitals of Möbius-type conformations of annulenes, *Tetrahedron Lett.* **5** (1964) 1923–1928.

[13] H. E. Zimmerman, On molecular orbital correlation diagrams, the occurrence of Möbius systems in cyclization reactions, and factors controlling ground and excited state reactions. I & II, *J. Am. Chem. Soc.* **88** (1966) 1564–1565, 1566–1567.

[14] R. F. Langler, Salgado, C. Mendizabal, Hückel and Möbius annulenes: Relationships between their Hückel-level orbitals and their Hückel-level energies, *Quimica Nova* **23** (2000) 841–844.

[15] P. W. Fowler, Hückel spectra of Möbius π systems, *Phys. Chem. Chem. Phys.* **4** (2002) 2878–83.

[16] J. Stillwell, *Classical Topology and Combinatorial Group Theory*, 2nd edition, Springer, New York, 1993.

[17] See, e.g., H. Hosoya, F. Harary, On the matching properties of three fence graphs, *J. Math. Chem.* **12** (1993) 211–218.

[18] P. W. Fowler, B. T. Pickup, T. Z. Todorova, Möbius devices: a twist in the tale of molecular conduction, (To be published).

[19] I. Gutman, Spectral properties of some graphs derived from bipartite graphs, *MATCH Commun. Math. Comput. Chem.* **8** (1980) 291–314.

[20] E. Estrada, Generalized walks-based centrality measures for complex biological networks, *J Theor Biol.* **263** (2010) 556–565.

[21] V. Ejov, J. A. Filar, S. K. Lucas, P. Zograf, Clustering of spectra and fractals of regular graphs, *J. Math. Anal. Appl.* **333** (2007) 236–246.